



Measuring pelvises in 3D surface scans and in MDCT generated virtual environment: Considerations for applications in the forensic context

Claudine Abegg^a, Fatbardha Hoxha^{b,c}, Lorenzo Campana^a, Oguzhan Ekizoglu^{c,d},
Sami Schranz^c, Coraline Egger^c, Silke Grabherr^{a,c}, Marie Besse^b, Negahnaz Moghaddam^{a,e,*}

^a Unit of Forensic Imaging and Anthropology, University Centre of Legal Medicine Lausanne-Geneva, Lausanne University Hospital and University of Lausanne, Switzerland

^b Laboratory for Prehistoric Archaeology and Anthropology, Department F.-A. Forel for Environmental and Aquatic Sciences, Faculty of Science, University of Geneva, Switzerland

^c Unit of Forensic Imaging and Anthropology, University Centre of Legal Medicine Lausanne-Geneva, Geneva University Hospital and University of Geneva, Switzerland

^d Tepecik Training and Research Hospital, Department of Forensic Medicine, Izmir, Turkey

^e Swiss Human Institute of Forensic Taphonomy, University Centre of Legal Medicine Lausanne-Geneva, Lausanne University Hospital and University of Lausanne, Switzerland

ARTICLE INFO

Keywords:

Virtual Anthropology
Morphometrics
Diagnose Sexuelle Probabiliste
Ischio-Pubic Index
Pelvis
Computed Tomography
3D Surface Scans

ABSTRACT

Virtual Anthropology (VA) transposes the traditional methods of physical anthropology to virtual environments using imaging techniques and exploits imaging technologies to devise new methodological protocols. In this research, we investigate whether the measurements used in the Diagnose Sexuelle Probabiliste (DSP) and Ischio-Pubic Index (IPI) differ significantly when 3D models of a bone are generated using 3D surface scans (3DSS) and Multidetector Computed Tomography (MDCT) scans. Thirty pelvises were selected from the SIMON identified skeletal collection. An equal ratio of females to males was sought, as well as a good preservation of the bones. The pelvises were scanned using an MDCT scanner and a 3D surface scanner. The measurements of the DSP and IPI methods on the dry bones (referred to as macroscopic measurements here), and then to the 3D models. The intra- and interobserver, using the Technical Error of Measurement (TEM) and relative Technical Error of Measurement (rTEM) error was assessed, and we aimed to observe if the measurements made on the MDCT and 3DSS generated models were significantly different from those taken on the dry bones. Additionally, the normality of the data was tested (Shapiro-Wilk test) and the differences in measurements was evaluated using parametric (Student t-tests) and non-parametric (Wilcoxon) tests. The TEM and rTEM calculations show high intra and interobserver consistency in general. However, some measurements present insufficient inter- and intraobserver agreement. Student t and Wilcoxon tests indicate potentially significant differences of some measurements between the different environments. The results show that especially in the virtual environment, it is not easy to find the right angle for some of the DSP measurements, However, when comparing the measurement differences between dry and virtual bones, the results show that most of the differences are less than or equal to 2.5 mm. Considering the IPI, the landmarks are already difficult to determine on the dry bone, but they are even more difficult to locate in the virtual environment. Nevertheless, this study shows that quantitative methods may be better suited for application in the virtual environment, but further research using different methods is needed.

1. Introduction

Virtual anthropology (VA), as a discipline and a technique, presents numerous advantages. It allows for less manipulation of the skeletal remains, re-examination long after the bones might have been buried or

destroyed, or the visualisation of different kind of data than is available to the naked eye (densitometry in MDCT scans, for example) [1]. As such, it answers many imperatives of forensic data: the possibility to re-visit conclusions based on renewed observation and minimizing risk of destroying evidence through manipulation.

* Correspondence to: Unit of forensic imaging and anthropology, Swiss Human Institute of Forensic Taphonomy, Chemin de la Vulliette 4, CH - 1000 Lausanne 25, Switzerland.

<https://doi.org/10.1016/j.forensiint.2023.111813>

Received 14 November 2022; Received in revised form 18 July 2023; Accepted 26 August 2023

Available online 1 September 2023

0379-0738/© 2023 The Authors. Published by Elsevier B.V. This is an open access article under the CC BY license (<http://creativecommons.org/licenses/by/4.0/>).

From an academic perspective, virtual anthropology permits a more democratic access to skeletal data in research, when in the past such access was defined by the student / researcher's location (access to local collections) or the ability to travel to where skeletal collections are held. This last characteristic of virtual anthropology was particularly highlighted during the COVID-19 pandemic, when research worldwide was considerably slowed down [2] and differential access to skeletal material was starkly felt by those in institutions that possess no such collections.

In the forensic context, forensic anthropologists assist in the process of the identification of unknown human remains. The reconstruction of the biological profile includes the estimated age-at-death, sex, and stature of the deceased. Due to its biological function, the pelvic bone provides distinct sexual dimorphism and thus is the most important skeletal element when it comes to sex estimation of an unknown human remains [3–7]. Various morphological [8–10] and morphometric traits [11–15] for sex estimations on the os coxae were identified and in the last decades numerous research projects have focused on the enhancement of known methods but also the development of new methods. Virtual anthropology offers new opportunities for forensic anthropology, but comes with some pitfalls, as seen above. One of the major obstacles to its systematic application within forensic anthropology, is the question of whether the “traditional” methods of physical anthropology are readily applicable to virtual environments. In recent years, data has been published attempting to compare anthropological methods on dry bones (or replicates) and virtual environment [16–22]. Research has been conducted on the sex estimation on the pelvic bones in virtual environment, including analyses on 3D models [18]. But the question remains, are anthropologists, who are used to visualising and measuring the actual bones in their hands consistent when applying these same methods in virtual settings? Are comparable results observed? Answering these questions is of crucial importance; if the results obtained using the traditional anthropological methods cannot be replicated in a virtual setting, then the method must be discarded for use in these particular circumstances, and new ones devised. The research presented here builds upon previous investigations into the applicability of methods from “traditional” anthropology into virtual environments [16]. The aim of the presented research was to investigate how measurements taken in three different environments – on dry bones (macroscopy), on 3D models reconstituted from CT scans, and on 3D surface scans (3DSS) – compared to one another, to determine whether these two virtual environments (CT and 3DSS) are suitable for Virtual Anthropology. In order to be able to quantify variations, morphometric traits were used. Measurements issued from two sex determination methods, the Diagnose Sexuelle Probabiliste (DSP) and the Ischio-Pubic Index (IPI) were used.

2. Materials and methods

2.1. Materials

2.1.1. The SIMON Identified Skeletal Collection sample

The SIMON Identified Skeletal Collection, or SIMON collection, is as its name indicates a reference collection housed at the University of Geneva, Switzerland. The SIMON Identified Skeletal collection is comprised of 496 individuals, including 204 women, 292 men, and 16 subadults [23]. The collection was first created in 1991, thanks to a Swiss National Science Foundation (SNFS) grant to Christian Simon, in order for a PhD student (Isabelle Gemmerich) to constitute an identified collection for her research. The collection is issued from late 19th-early 20th century tombs from cemeteries of the Vaud canton. Permission to constitute the skeletal collection was sought and granted from cantonal authorities, municipal authorities, and surviving family of the individuals [23]. In 1998, a new project was granted to continue the original collection. The collection was named SIMON identified skeletal collection after Christian Simon's demise in 2000. The parameters of the

individuals chosen are given in Table 1 below.

The skeletons of all 30 individuals were fully MDCT scanned (parameters given below) and then the pelvises were scanned using a 3D surface scanner. One right pelvis could not be surface scanned due to organizational reasons. A total of 60 dry pelvises, 60 CT images and 59 surface scans were used for the analyses. Outside of the initial selection of individuals by observer 1 based on the preservation of the pelvises, no identifying information was available to the observers during the duration of the experiment.

3. Methods

3.1. The ischio-pubic index (IPI)

The IPI was developed by Schultz and published in 1930 [24]. On the os coxae, he focused on the measurements of the pelvis (Fig. 1) and argued that it could be used to determine whether a species could be bipedal or not. Later, two of the measurements were investigated by Washburn [25] (length of the pubis “OA”, and length of the ischium, “OB” in Fig. 1) to devise an index, which could be used to determine the sex of human skeletal remains. This index has sometimes been used in archaeological or forensic cases [26,27].

3.2. The diagnose sexuelle probabiliste (DSP)

The Diagnose Sexuelle Probabiliste (DSP) is a method developed by Murail, Brůžek [15] based on 10 measurements taken on the os coxae (Table 2). A minimum of four measurements is needed for a sex estimation to be given by the software, which is freely available [12]. The 10 measurements to be taken are described in Table 2. All 10 measurements were considered. When used to sex pelvises, the method reports an accuracy ranging from 98.7% to 99.63%, depending on the population tested [15].

3.3. CT scans

The MDCT scans were performed on a sixty four-row MDCT unit (CT VTC; GE Healthcare, Milwaukee, WI, USA); Matrix: 512; Field of view: Variable, depending on the object section 25–50 cm; Slice thickness: 0.625 mm; Reconstruction interval: 0.3 mm; 100 kv and 120 mA; tube rotation 1 s; pitch 1.375. Two types of reconstruction were applied (Reconstruction Type 1: Standard; Thickness 0.625; Interval 0.3; Reconstruction Type 2: Bone Plus; Thickness 0.625; Interval 0.3).

Image viewing and post processing were done using GE AW Server 3.2 Ext 4.0 (GE Healthcare, Milwaukee, WI, USA). In order to secure the bones during movement of the CT-table, as well as to ensure good segmentation of the bones afterwards for research, the skeleton was laid on radio translucent material, with cut-outs specific to each bone type in order to retain anatomical position as much as possible (Fig. 2). VR (volume rendering) models were generated from the Standard reconstructions in the GE AW Server 3.2 Ext 4.0 (GE Healthcare, Milwaukee, WI, USA) system, and visualised in its “3D reconstruction” panel. Measurements were taken directly in this environment.

Table 1

Parameters of the individuals chosen for analysis within the Simon Identified Skeletal Collection.

Total number of individuals	30
Number of os coxae (one left and one right for each individual)	60
Male individuals	15
Female individuals	15
Average age at death (years)	43
Youngest individual	18
Oldest individual	83

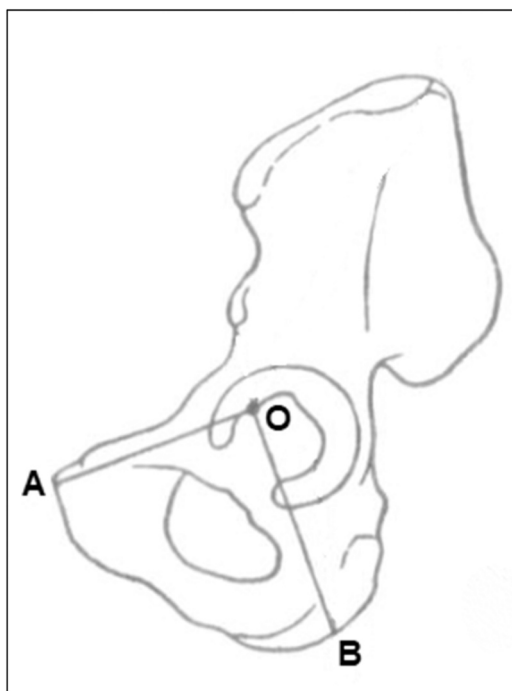


Fig. 1. Measurements on the coxal according to Schultz [24], p- 346, modified by the authors to illustrate the measurements taken for this study. The ischium is represented by measure OB, the pubis by measure OA.

Table 2
Description of the measurements of the DSP, adapted from Murail, Brůžek [15].

Measure name	Description
PUM	Acetabulo-symphyseal pubic length: Minimum distance from the superior and medial point of the pubic symphysis to the nearest point on the acetabular rim at the level of the lunate surface (M 14 -[28])
SPU	Cotylo-pubic breadth: Pubic breadth between the most lateral acetabular point and the medial aspect of the pubis. Measurement is perpendicular to the major axis of the os pubis. Arms of the sliding caliper are thus parallel to the plane of the obturator foramen ([29])
DCOX	Maximum pelvic height: Maximum height of os coxae measured from the inferior border of the os coxae to the most superior portion of the iliac crest. Can be taken with sliding calipers or osteometric board (M1 -[28])
IIMT	Depth of the great sciatic notch: Distance from the postero-inferior iliac spine (defined as the point of intersection between the auricular surface and the posterior portion of the sciatic notch) to anterior border of the great sciatic notch. Axis of the measurement must be perpendicular to the anterior border. Because of the configuration of hip bone, it is easier to use small arms of sliding caliper (M 15.1 -[28])
ISMM	Post-acetabular ischium length: Distance from the most anterior and inferior point of the ischial tuberosity to the furthest point on the acetabular border ([30]- IT - A)
SCOX	Iliac breadth: Distance between the anterior-superior iliac spine and the postero-superior iliac spine (M 12 -[28])
SS	Spino-sciatic length: Minimum distance between the antero-inferior iliac spine and the deepest point in the greater sciatic notch ([29])
SA	Spino-auricular length: Distance between the antero-inferior iliac spine and the auricular point. Auricular point is defined as the intersection of the arcuate line with the auricular surface ([29])
SIS	Cotylo-sciatic breadth: Distance between the lateral border of the acetabulum and the midpoint of the anterior portion of the great sciatic notch. Fixed arm of the sliding caliper is parallel to the acetabular plane (M 14.1 -[28])
VEAC	Vertical acetabular diameter: Maximum vertical diameter of the acetabulum, measured on the acetabular rim, as a prolongation of the longitudinal axis of the ischium (M 22 -[28])



Fig. 2. MDCT of an individual of the SIMON collection set up for pelvis scanning (image taken at the University Center of Legal Medicine Geneva).

3.4. 3D surface scans

For the surface scan the handheld scanner Go!SCAN 20 from Creaform was used. This scanner is based on structured light, projecting a pattern similar to a QR code over the object being scanned. Two cameras observe the distortion of the pattern on the object so that the software can calculate 3D coordinates on the surface corresponding to every pixel of the cameras. The device acquires 550 000 image pairs per second and has a scanning area of 143 × 108 mm. A third camera captures the colour of the scanned surface. More detailed parameters are available in Table 3.

3.5. Measurement process

Two observers (OBS1 and OBS2) were mobilised for the analyses in an observer-blind study. One has over 10 years' experience in anthropology, the other is a student undergoing their first year of training and learning the methods specifically for the study. The latter had the opportunity to train on a few pelvises and to discuss any questions regarding taking measurement with the more experienced researcher during a training session that took place a few weeks before the first rounds of measurements. Both observers were trained in the analyses of the virtual bones prior to the study. The observers took a first round of measurements manually, on the dry bones, independently from one another, on both the right and left pelvis of each individual. Several days later, the observers took a first round of measurements on the 3D models generated from the 3DSS. Finally, the same measurements were taken on the MDCT-generated models. A break of two weeks was then taken, after which the entire operation was repeated. Fig. 3 shows an example of measurements taken in the 3D surface scan and MDCT-scan environments.

3.6. Data analysis

All data was analysed in Jamovi and Microsoft Excel. The Technical Error of Measurement (TEM), relative TEM (rTEM), the Shapiro-Wilk test for normality as well as parametric (Student t-tests) and non-

Table 3
Surface scanner parameters (adapted from Creaform Go!SCAN 3D devices brochure).

Creaform Go!SCAN 20 Technical Specification	
Accuracy	Up to 0.100 mm (0.004 in.)
Volumetric accuracy	0.300 mm/m (0.0036 in./ft)
Resolution	0.100 mm (0.004 in.)
Measurement rate	550,000 measurements/s
Scanning area	143 × 108 mm (5.6 in x 4.3 in)
Depth of field	100 mm (4 in.)
Recommended Part size range	0.05–0.5 m (2–20 in.)

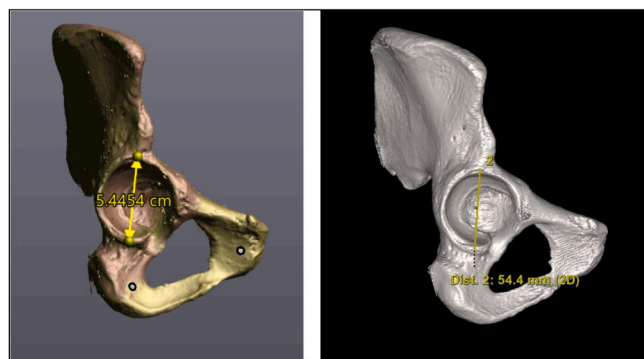


Fig. 3. Examples of a DSP measurement (VEAC) taken on the same pelvis on a model created from a 3D surface scan (left, in cm) and a MDCT scan (right, in mm).

parametric (Wilcoxon-Mann-Whitney tests) paired sample t-tests were used to scrutinize the data. The significance value chosen for the tests was 0.05, meaning the null hypothesis (no differences between the different environments) is rejected for p values less than 0.05.

4. Results

All raw data and results tables are available as [Supplementary materials](#) (Suppl. 1 and 2).

Descriptive statistics (n = number of cases, mean, max = maximum, min = minimum) of all individual measurements of the DSP and the IPI for both rounds of OBS 1 and OBS2 in all three environments are shown in supplementary 3.

4.1. Intra- and interobserver assessment – TEM and rTEM

In order to assess the intra- and interobserver error, the Technical Error of Measurement (TEM) and relative Technical Error of Measurement (rTEM) were calculated according to the principles outlined in [31], in Excel. Both observers conducted two rounds of observation in each visual medium, measuring all pelvises. The TEM calculation is a descriptive statistic quantifying the difference between two repeated measurements, and the rTEM expresses that difference as a percentage so that it may be compared across various measurements [31–33]. The percentage at which the rTEM is considered too high to be insignificant is set at 5%, as shown in previous publications [31,34].

Intraobserver error were calculated using all measurements from the first and second round of observations for both observers individually. Interobserver error was calculated using all first round measurements of both observers. Intra and interobserver error of the DSP individual measurements for each environment are shown in Table 4 for the dry bone analyses (macro), in Table 5 for the CT image analyses, and in Table 6 for surface scan analyses (3D). Intra and interobserver error of

Table 4

Intra and Interobserver error of OBS1 and OBS2 for the DSP measurements on the dry bone (macro). The rTEM values above 5% are shown in bold.

MACRO DSP	Intraobserver (OBS1)			Intraobserver (OBS2)			Interobserver		
	TEM	rTem	R	TEM	rTem	R	TEM	rTem	R
PUM	1.93	2.64	0.85	1.59	2.19	0.88	2.19	3.04	0.79
SPU	3.77	13.95	0.53	0.97	3.56	0.95	1.79	6.68	0.82
DCOX	2.88	1.38	0.95	2.33	1.09	0.96	3.67	1.74	0.92
IIMT	3.72	8.64	0.70	1.68	3.93	0.92	2.97	7.08	0.78
ISMM	0.66	0.60	0.99	0.77	0.70	0.99	1.20	1.10	0.98
SCOX	2.49	1.60	0.89	2.39	1.53	0.90	2.84	1.82	0.87
SS	0.95	1.29	0.96	0.82	1.11	0.97	1.18	1.60	0.94
SA	1.18	1.51	0.96	1.76	2.24	0.90	1.21	1.55	0.95
SIS	0.46	1.20	0.99	0.70	1.81	0.96	0.89	2.30	0.94
VEAC	0.73	1.32	0.97	0.85	1.50	0.96	1.30	2.33	0.90

the IPI individual measurements for each environment are listed in Table 7.

4.2. Inferential statistics

Additional inferential statistics were performed on the data of OBS 1 in order to further analyse the differences in the measurements taken in the various environments.

The normality of the data was tested for both the DSP measurements and the IPI measurements. The Shapiro-Wilk test was applied to each set of measurements, revealing that some measurements were normally distributed, and others not (Suppl. 4).

As a result, both Wilcoxon-Mann-Whitney tests (non-parametric) and Student t-tests were applied to the data. Additionally, non-parametric tests, such as the Wilcoxon test consider outliers. This was detected in the VEAC measurement of the left pelvis of AIG_16.

First, both the DSP and IPI data were subjected to Wilcoxon-Mann-Whitney test to see if there were significant differences in the measurements taken on the bones (macro), on the CT reconstruction, and on the 3DSS (Tables 8 and 9).

Additional statistical tests were performed in order to evaluate the individual measurements within the DSP and IPI method. Each of the different measurements taken on the bones, for each method, were tested against their paired data in the CT and 3DSS environments, in order to determine whether a few of the measurements could be inducing major differences.

Student t-test and Wilcoxon W test for the individual DSP and IPI measurements in macro, CT, and 3DSS environments are shown in Table 10 and Table 11.

4.3. Range of differences in measurements

The data from OBS 1 was arranged so that the differences between each paired measurements was calculated, made absolute, and then classified into the following ranges: “less or equal to 2.5 mm”, “greater than 2.5 mm, less or equal to 5 mm”, “more than 5 mm and less or equal to 10 mm”, and “greater than 10 mm”, as a logical mathematical progression. The number of occurrences in each category of the scale was then expressed as a percentage of the total number of paired measurements taken, in order for the results to be comparable across DSP and IPI. Figs. 4–6 present the results of this analysis for each measurement.

4.4. Sex estimation using metric data

To evaluate the effect of the measurement differences, the final sex estimates of the pelvic bones are shown in Figs. 7 and 8. Since the aim of the study was not to assess the individual sex estimation methods, the analyses focused on determining the correct, undetermined and incorrect sex evaluation in order to analyse the impact of the above-mentioned range of differences in measurements.

The pelvises for which the IPI measurements could not be taken for

Table 5

Intra and Interobserver error of OBS1 and OBS2 for the DSP measurements on the CT images. The rTEM values above 5% are shown in bold.

CT DSP	Intraobserver (O1)			Intraobserver (O2)			Interobserver		
	TEM	rTem	R	TEM	rTEM	R	TEM	rTEM	R
PUM	1.71	2.35	0.88	2.11	2.92	0.80	2.02	2.80	0.82
SPU	0.71	2.42	0.97	1.16	4.14	0.92	1.29	4.51	0.91
DCOX	4.83	2.30	0.86	2.38	1.14	0.96	4.36	2.08	0.89
IIMT	3.81	8.60	0.58	1.59	3.87	0.90	4.07	9.56	0.48
ISMM	1.69	1.57	0.96	3.42	3.24	0.85	3.48	3.27	0.84
SCOX	1.74	1.11	0.95	3.35	2.16	0.85	3.33	2.14	0.85
SS	1.47	2.00	0.92	1.03	1.38	0.95	1.59	2.14	0.89
SA	2.19	2.88	0.82	2.14	2.71	0.86	3.63	4.69	0.54
SIS	0.63	1.61	0.97	0.97	2.51	0.93	0.96	2.45	0.93
VEAC	1.22	2.24	0.93	1.25	2.31	0.91	1.33	2.46	0.91

Table 6

Intra and Interobserver error of OBS1 and OBS2 for the DSP measurements of the 3D scans. The rTEM values above 5% are shown in bold.

3D DSP	Intraobserver (O1)			Intraobserver (O2)			Interobserver		
	TEM	rTem	R	TEM	rTEM	R	Tem	rTEM	R
PUM	1.26	1.74	0.95	1.37	1.90	0.91	1.56	2.19	0.91
SPU	1.74	6.08	0.85	1.70	6.21	0.87	1.89	6.77	0.81
DCOX	18.80	8.99	0.25	1.53	0.72	0.99	18.46	8.84	0.26
IIMT	2.56	5.56	0.76	1.43	3.43	0.93	4.14	9.58	0.43
ISMM	2.86	2.61	0.89	0.81	0.74	0.99	1.08	0.99	0.98
SCOX	1.33	0.85	0.97	1.99	1.28	0.94	1.54	0.99	0.96
SS	1.56	2.13	0.89	1.02	1.37	0.96	1.19	1.61	0.93
SA	1.19	1.52	0.96	1.28	1.63	0.95	1.33	1.70	0.95
SIS	0.76	1.99	0.96	1.20	3.13	0.91	0.86	2.23	0.95
VEAC	6.64	11.73	0.25	0.77	1.39	0.97	6.94	12.35	0.19

Table 7

Intra and Interobserver error of OBS1 and OBS2 for the IPI measurements for all three environments (macro, CT images, and 3D scans). The rTEM values above 5% are shown in bold.

IPI		Intraobserver (O1)			Intraobserver (O2)			Interobserver		
		TEM	rTem	R	TEM	rTEM	R	TEM	rTem	R
MACRO	OA	2.66	3.48	0.79	2.84	3.45	0.73	3.71	4.77	0.63
	OB	2.57	3.16	0.83	2.89	3.45	0.82	2.91	3.55	0.78
CT	OA	3.47	4.68	0.66	3.50	4.36	0.70	4.91	6.35	0.36
	OB	3.65	4.48	0.70	3.81	4.55	0.68	3.19	3.88	0.77
3D	OA	1.47	2.02	0.94	2.65	3.24	0.77	6.82	8.77	-0.32
	OB	3.26	4.08	0.71	2.40	2.86	0.90	4.39	5.40	0.57

Table 8

Wilcoxon test comparing the IPI measurements taken in macro, CT, and 3DSS environments, for both observer and both rounds of observation. The values in bold indicate a p value less than 0.05.

			statistic	p value
OBS1_IPI_MACRO	OBS1_IPI_3D	Wilcoxon W	12884	< .001
	OBS1_IPI_CT	Wilcoxon W	10330	0.012
OBS1_IPI_3D		Wilcoxon W	6627	0.007

Table 9

Wilcoxon test comparing the DSP measurements taken in macro, CT, and 3DSS environments. The values in bold indicate a p value less than 0.05.

			statistic	p value
OBS1_DSP_MACRO	OBS1_DSP_3D	Wilcoxon W	207847	< .001
	OBS1_DSP_CT	Wilcoxon W	67709	0.026
OBS1_DSP_3D		Wilcoxon W	89202	< .001

sex estimation were marked as not observable.

5. Discussion

There are several important points to raise in this discussion. First, it

is worth mentioning again that the aim of this analysis was to investigate the potential differences in measurements taken in different environments: macroscopically (on the dry bone), on reconstructions from CT scans, and from 3DSS. The authors did not aim to assess the methods (DSP and IPI) from which these measurements are taken; the methods

Table 10

Student t-test and Wilcoxon W test for the individual DSP measurements in macro, CT, and 3DSS environments. The values in bold indicate a p value less than 0.05 (df = degree of freedom).

PUM	test	Statistic	df	p value	
PUM_MACRO	PUM_3D	Student t-test	2.237	83	0.028
		Wilcoxon W	2676		< .001
PUM_CT		Student t-test	1.129	86	0.262
		Wilcoxon W	2205 ^a		0.036
PUM_3D		Student t-test	-0.932	89	0.354
		Wilcoxon W	1745		0.224
^a 4 pair(s) of values were linked					
SPU	test	Statistic	df	p value	
SPU_MACRO	SPU_3D	Student t-test	-3.23	104	0.002
		Wilcoxon W	781		< .001
SPU_CT		Student t-test	-5.09	105	< .001
		Wilcoxon W	173 ^a		< .001
SPU_3D		Student t-test	-3.08	102	0.003
		Wilcoxon W	890 ^a		< .001
^a 1 pair(s) of values were linked					
DCOX	test	Statistic	df	p value	
DCOX_MACRO	DCOX_3D	Student t-tests	0.235	112	0.815
		Wilcoxon W	1807		< .001
DCOX_CT		Student t-tests	-1.367	114	0.174
		Wilcoxon W	2172		0.001
DCOX_3D		Student t-tests	-0.731	113	0.466
		Wilcoxon W	2930 ^a		0.406
^a 1 pair(s) of values were linked					
IIMT	test	Statistic	df	p value	
IIMT_MACRO	IIMT_3D	Student t-test	-5.98	112	< .001
		Wilcoxon W	1117		< .001
IIMT_CT		Student t-test	-2.14	115	0.035
		Wilcoxon W	2471 ^a		0.023
IIMT_3D		Student t-test	4.03	113	< .001
		Wilcoxon W	4777		< .001
^a 2 pair(s) of values were linked					
ISMM	test	Statistic	df	p value	
ISMM_MACRO	ISMM_3D	Student t-test	-1.69	111	0.094
		Wilcoxon W	1559		< .001
ISMM_CT		Student t-test	7.45	113	< .001
		Wilcoxon W	5636		< .001
ISMM_3D		Student t-test	6.46	113	< .001
		Wilcoxon W	5980		< .001
SCOX	test	Statistic	df	p value	
SCOX_MACRO	SCOX_3D	Student t-test	-4.95	96	< .001
		Wilcoxon W	961		< .001
SCOX_CT		Student t-test	-6.44	98	< .001
		Wilcoxon W	881		< .001
SCOX_3D		Student t-test	-1.24	99	0.219
		Wilcoxon W	2017		0.081
SS	test	Statistic	df	p value	
SS_MACRO	SS_3D	Student t-test	1.358	115	0.177
		Wilcoxon W	4159		0.035
SS_CT		Student t-test	-0.377	117	0.707
		Wilcoxon W	2938 ^a		0.512
SS_3D		Student t-test	-1.279	117	0.204
		Wilcoxon W	2646		0.020
^a 6 pair(s) of values were linked					
SA	test	Statistic	df	p value	
SA_MACRO	SA_3D	Student t-test	0.956	113	0.341
		Wilcoxon W	4017 ^a		0.023
SA_CT		Student t-test	7.794	115	< .001
		Wilcoxon W	5840		< .001
SA_3D		Student t-test	7.728	115	< .001
		Wilcoxon W	5798		< .001
^a 1 pair(s) of values were linked					
SIS	test	Statistic	df	p value	
SIS_MACRO	SIS_3D	Student t-test	2.4	115	0.018
		Wilcoxon W	4720		< .001
SIS_CT		Student t-test	-5.1	115	< .001
		Wilcoxon W	1279 ^a		< .001
SIS_3D		Student t-test	-7.39	113	< .001
		Wilcoxon W	763		< .001
^a 11 pair(s) of values were linked					
VEAC	test	Statistic	df	p value	
VEAC_MACRO	VEAC_3D	Student t-test	-2.32	117	0.022

Table 10 (continued)

PUM	test	Statistic	df	p value
VEAC_CT	Wilcoxon W	1448		< .001
	Student t-test	6.94	119	< .001
VEAC_3D	Wilcoxon W	6005 ^a		< .001
	Student t-test	3.82	117	< .001
	Wilcoxon W	6555		< .001
^a 2 pair(s) of values were linked				

Table 11

Student t-test and Wilcoxon W test for the individual IPI measurements in macro, CT, and 3DSS environments. The values in bold indicate a p value less than 0.05 (df = degree of freedom).

OA	test	Statistic	df	p value	
OA_MACRO	OA_3D	Student t-test	6.18	82	< .001
		Wilcoxon W	3002		< .001
OA_CT		Student t-test	4.38	84	< .001
		Wilcoxon W	2712 ^a		< .001
OA_3D		Student t-test	-1.4	88	0.164
		Wilcoxon W	1642		0.141
OB	test	Statistic	df	p value	
OB_MACRO	OB_3D	Student t-test	2.732	106	0.007
		Wilcoxon W	3589		0.03
OB_CT		Student t-test	-0.664	109	0.508
		Wilcoxon W	2843 ^a		0.64
OB_3D		Student t-test	-3.08	111	0.003
		Wilcoxon W	2347		0.018
^a 1 pair(s) of values were linked					

are well known and already widely discussed in existing anthropological literature [12,15,26,27,35–37].

The Technical Error of Measurement (TEM) and relative TEM (rTEM) calculations show that the intra- and interobserver error was generally low. However, some of the DSP measurements show poor inter- and intraobserver agreement. This can be observed for SPU and IIMT in the macro observations; IIMT on the CT images; SPU, DCOX, IIMT and VEAC on the 3D scans. The rTEM values of 13.9% for SPU Macro, 11.7% for VEAC 3D, and 8.99% for DCOX 3D observed for the intraobserver agreement of OBS1 may be also explained due to errors in the entry (OBS1_Round 2_SPU_macro = 68.8 mm; OBS1_Round 1_VEAC_3D scan = 113.1 mm, OBS1_DCOX_3D scan = 22.65 mm; see suppl. 1). However, the IIMT measurement, which show rTEM values above 5% in all three environments, can rather be explained by the difficulty of the measurement.

We further examined the data of OBS1 by comparing pair-matched data across the different visual environments, using Student t-test and Wilcoxon tests. The results suggest potentially significant differences in some measurements taken. For some measurements the right angle was difficult to find, especially in the virtual environment. As mentioned, the IIMT in particular proved to be a difficult measurement. In a similar research on archaeological material, the definition of the IIMT measurement was adapted for the purpose of the research aim, which eventually reduced the previous obtained high rTEM value to below 5% [17].

The analyses indicated that some measurements might be easier to take than others, due to the type of landmarks that must be identified to take the measure correctly, leading to a wider range of results. To investigate this hypothesis, each type of measurement taken was tested across the three visual environments. This revealed that some measurements lack concordance across the different visual mediums (e.g. SPU, IIMT, and SIS from the DSP), whilst others (e.g. DCOX and SS from the DSP) yield better results across the board (Table 10).

Nevertheless, these results raised the question of the scale of differences in measurements. This was important to investigate, as most methods can tolerate a small uncertainty in measurements but repeated large errors should raise a red flag as to the method's applicability in any

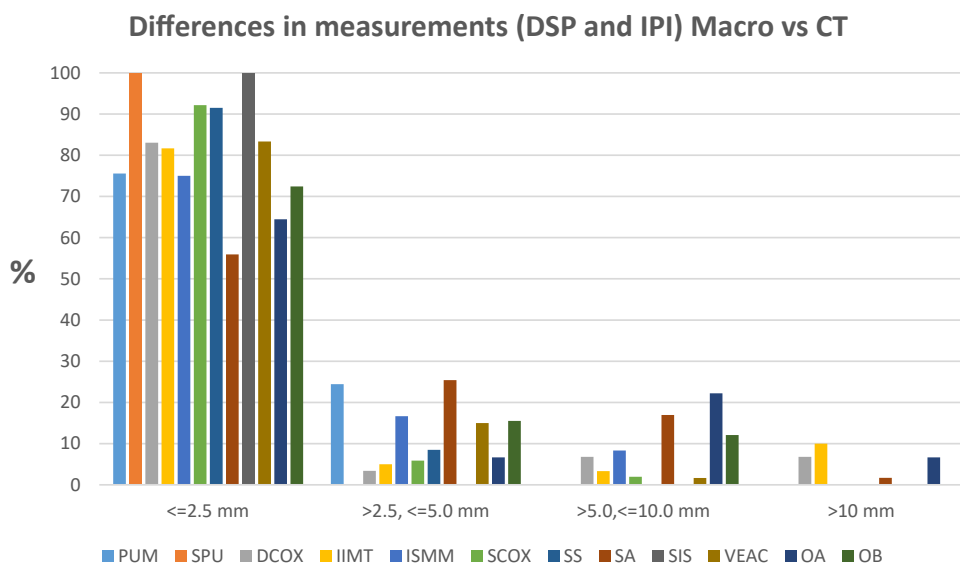


Fig. 4. Proportion (in %) of repeated measurements falling within the categories “less or equal to 2.5 mm”, “greater than 2.5 mm, less or equal to 5 mm”, “more than 5 mm and less or equal to 10 mm”, and “greater than 10 mm” for the DSP and IPI measurements comparing macro and CT.

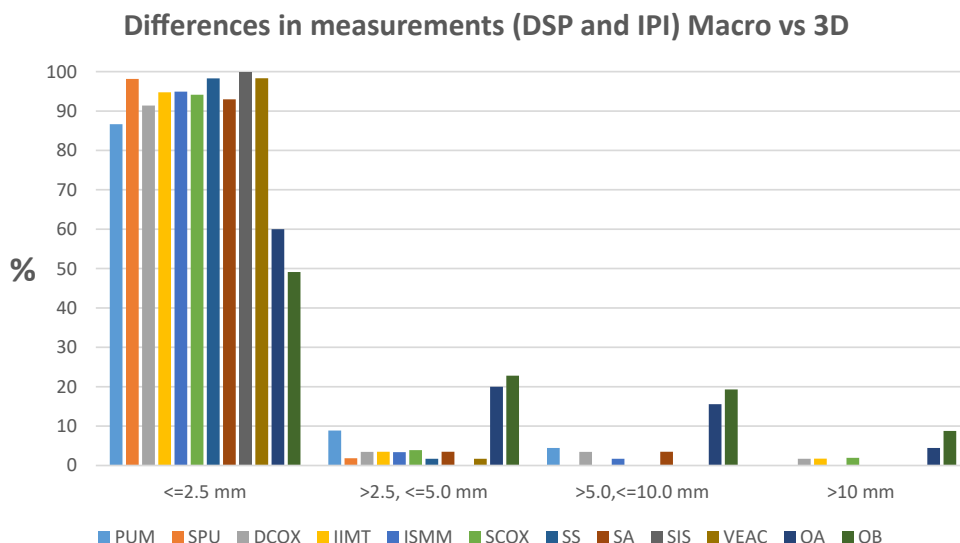


Fig. 5. Proportion (in %) of repeated measurements falling within the categories “less or equal to 2.5 mm”, “greater than 2.5 mm, less or equal to 5 mm”, “more than 5 mm and less or equal to 10 mm”, and “greater than 10 mm” for the DSP and IPI measurements comparing macro and 3D.

context. Looking at these differences in measurements, it appears that the DSP and the IPI fare very differently. For the DSP, the majority of the differences in measurements fall in the smallest category (less or equal to 2.5 mm) in all three environments. For the IPI, this distribution is not as clear (see suppl. 3). Although a large proportion of the measurement differences also falls into the smallest category, the measurement differences are spread across the different categories, especially for the measurements in the virtual environments. Since the effect of these measurement differences can vary, and 2.5 mm can have a greater impact on the outcome for short measurements than for long measurements, the impact on the final sex estimate was determined for the two methods. Analyses were performed on an identified skeletal collection so that the actual sex could be used to analyse the extend of the effect of measurement differences. The results show that for the DSP, these differences did not affect the final determination. Most of the pelvises analysed with the DSP measurements were correctly sexed (Fig. 7). This also suggests that “small” differences in measurements in the DSP measurements would not affect the applicability of the actual method.

Regarding the IPI measurement, it was not possible to obtain sufficient measurements for sex estimation in a number of cases, in all three environments and for both observers, which are noted as “not observable” (Fig. 8).

Whilst the results of this research suggest that quantitative, measurements-based methods appear to fare better in virtual environments than previously investigated qualitative methods [16], there are further aspects to be discussed. Not all measurements are equal, and the observers noted during the data collection process that the landmark “O” for the IPI measurements was difficult to identify macroscopically, also difficult in the 3DSS environment, and close to impossible to distinguish in most cases of CT scan reconstructions. This might explain the low interobservers agreement for the OA measurement especially on the surface scans. The difficulty in determining the exact measuring points was also described by Drew [26]. For the DSP it seems the anatomical landmarks were generally speaking easier to locate, but a few measurements proved repeatedly problematic and led to extensive discussions amongst the observers post data collection.

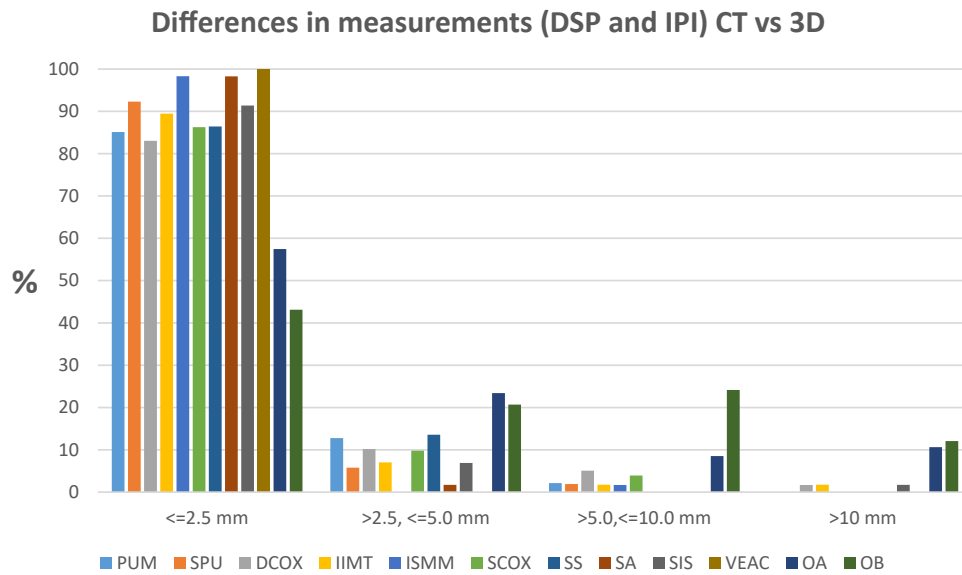


Fig. 6. Proportion (in %) of repeated measurements falling within the categories “less or equal to 2.5 mm”, “greater than 2.5 mm, less or equal to 5 mm”, “more than 5 mm and less or equal to 10 mm”, and “greater than 10 mm” for the DSP and IPI measurements comparing CT and 3D.

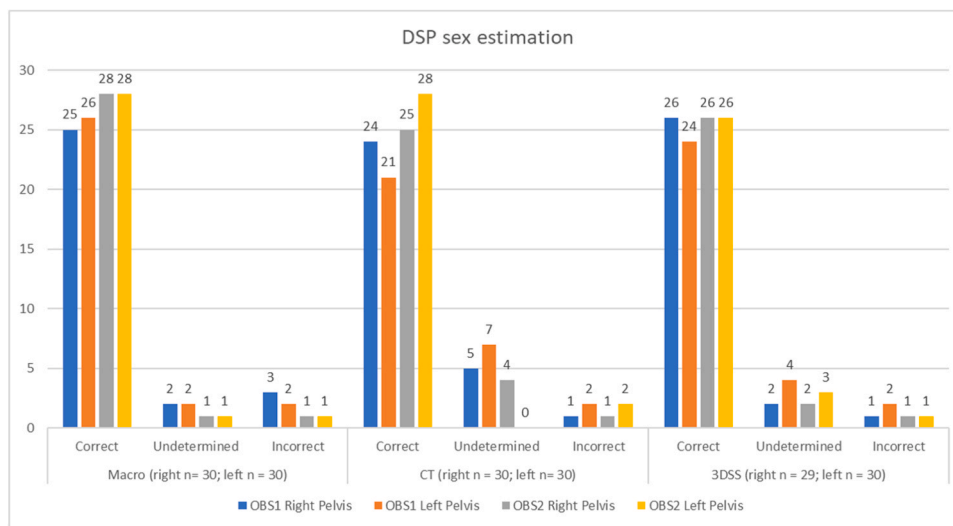


Fig. 7. Number of cases with correct, undetermined, and incorrect sex estimation by OBS1 and OBS2 using the DSP measurements (n = number).

Several wider issues must be raised based on these observations. First, one pitfall of such research is the tendency to equate all technologies. Indeed, as has been previously demonstrated [38], not all 3D imaging is equal. Comparing and contrasting results obtained on models generated by apparatus yielding wildly different accuracy introduces irreparable damage to the theoretical construct of the research. There are many types of MDCT scans and 3DSS, and dozens of accompanying software to create, analyse, and modify models. Whilst there are promising results as to the use of 3D models in VA [39,40] researchers should be attentive to the fact that the results obtained are valid for the models obtained with the apparatus, software, and parameters specified in each study. In this research, settings resulting in models of comparable resolution were used, which did not yield significant differences in measurements taken, as far as the DSP is concerned. It is important for readers to be aware that replicating the experiment with a different 3D surface scanner and different MDCT-scanner could yield different results. That is one of the pitfalls of Virtual Anthropology: results obtained are only valid in the particular settings in which they were acquired, and therefore many further experiments are necessary to ensure the viability

of the methods tested as tools for VA.

Furthermore, even though research has suggested that 3D-CT volume rendering images can be used for anthropometric analyses [18,41] it is important to point out that for radiologic diagnostics, 2D slices are used, as the virtual rendering of the CT data represent an interpolation of the slice samples. Indeed, as described by Stull, Tise [42], there are several reconstructing effects and visualisation biases when using 3D reconstructions from CT scans that can generate differences in the size of the virtual models, including for example variations due to the presence of soft tissues around the bone. Whilst these effects are well known by radiologists and medical imagery specialists, and understood by anthropologist, the question of whether anthropological methods, which are often more permissive than medical radiology ones in terms of measurement error can be applied on virtual reconstructions of bones still stands. In order to analyse a possible effect of the anthropometric measurements on 3D-CT volume rendering images in more detail, future studies could include the application of the measurements to 2D slices by a radiologist, which could be compared to the results obtained by anthropologists on the bones themselves and on 3D models.

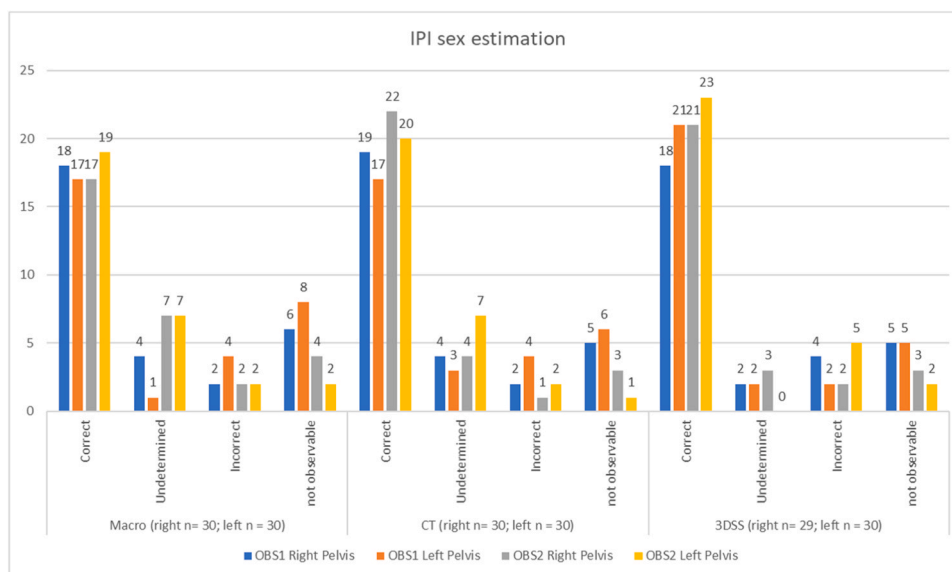


Fig. 8. Number of cases with correct, undetermined, and incorrect sex estimation by OBS1 and OBS2 using the IPI measurements (not observable = no IPI measurements could be taken for sex estimation, n = number).

Second, the redefinition of the role and training of forensic anthropologists as a logical consequence of the above should be mentioned. Whilst secondary education in physical anthropology is still very much a matter of learning the macroscopic analysis of skeletal human remains, as evidenced by textbooks on the topic [43–45], academic research in the discipline has evolved to include much more developed statistical and computer requirements. Some textbooks attempt to bridge this gap [46,47] but in many ways the knowledge required to operate scanners, generate data, and analyse models necessitate expertise from trained operators (3D engineers, radiological technicians, radiologists, statisticians, etc.). As anthropology becomes digital, it is also therefore becoming inherently interdisciplinary. Rather than a pitfall, this is a strength of the discipline, which does nonetheless rest upon clear communication of research objectives to all parties, so that the most appropriate apparatus and software is applied.

To summarise, a number of factors, including observer experience, the type of reconstitution and visualisation software used, or the method chosen for evaluation, could affect results obtained in virtual settings. The University Centre of Legal Medicine Lausanne-Geneva has long pioneered research on the application of forensic methods in virtual settings [16,39,40,48,49], and strives to investigate the potential of VA as a discipline, in collaboration with other institutions. Worldwide, research on age, sex, and stature determination in virtual settings is on the rise [21,50–53]. The number of methods to be tested, the need to access identified skeletal remains in order to accurately assess the results obtained by the observers against accurate information, and access to various means of generating 3D models (e.g. MDCT scans, 3DSS, photogrammetry) means there remains considerable work to be done on this topic.

6. Conclusions

Several conclusion can be drawn from this research. First, the DSP measurements seem to be well suited for the use in virtual environments, as they yielded mostly small differences in measurements. The same could not be said for the IPI, which appears to be difficult to apply in general. Quantitative methods might be better suitable for the application in the virtual environment, whilst appealing for more research on various methods in order to support or infer this theory. In the future, it would be useful to investigate how different apparatus influence the accuracy of measurements in Virtual Anthropology, by testing a range of

3DSS and software, for example. It would also be important to consider how other quantitative and qualitative methods that are recommended for biological profiling perform in a virtual environment.

CRedit authorship contribution statement

Abegg Claudine: Conceptualisation, Methodology, Formal analysis, Investigation, Writing – original draft, Writing – review & editing. **Hoxha Fatbardha:** Methodology, Formal analysis, Investigation, Data curation, Writing – review & editing. **Campana Lorenzo:** Methodology, Resources, Data curation, Writing – original draft, Writing – review & editing, Visualization. **Oguzhan Ekizoglu:** Data curation, Statistical analyses, Writing – review & editing. **Schranz Sami:** Methodology, Resources, Data curation, Writing – original draft, Writing – review & editing, Visualization. **Egger Coraline:** Resources, Writing – review & editing. **Graherr Silke:** Resources, Writing – review & editing, Supervision, Project administration. **Besse Marie:** Resources, Writing – review & editing, Supervision, Project administration. **Moghaddam Negahnaz:** Conceptualisation, Methodology, Writing – review & editing, Supervision, Project administration.

Declaration of Competing Interest

The authors declare that they have no known competing financial interests or personal relationships that could have appeared to influence the work reported in this paper.

Acknowledgements

The authors wish to thank all managers of the Simon Identified Skeletal Collection for access to the collection for this research project. We also wish to thank the anonymous reviewers, for their feedback and suggestions for improvements, and Silvia Bozza and Franco Taroni for their precious help in improving the statistics of this article. The authors furthermore would like to thank Clara Van Melle for her assistance in the editing process.

Appendix A. Supporting information

Supplementary data associated with this article can be found in the online version at [doi:10.1016/j.forsciint.2023.111813](https://doi.org/10.1016/j.forsciint.2023.111813).

References

- [1] G.W. Weber, F.L. Bookstein, *Virtual Anthropology: A Guide to A New Interdisciplinary Field*, Springer, 2011.
- [2] Rutherford, D. Funding Anthropological Research in the Age of Covid-19. 2020 [cited 2022 June 13]; Available from: (<https://americanethnologist.org/features/collections/covid-19-and-student-focused-concerns-threats-and-possibilities/funding-anthropological-research-in-the-age-of-covid-19>).
- [3] H. Correia, S. Balseiro, M. De Areia, Sexual dimorphism in the human pelvis: testing a new hypothesis, *Homo-J. Comp. Hum. Biol.* 56 (2) (2005) 153–160.
- [4] J.A. Gomez-Valdes, et al., Comparison of methods to determine sex by evaluating the greater sciatic notch: Visual, angular and geometric morphometrics, *Forensic Sci. Int.* 221 (2012) 1–3.
- [5] P.N. Gonzalez, et al., Analysis of dimorphic structures of the human pelvis: its implications for sex estimation in samples without reference collections, *J. Archaeol. Sci.* 34 (10) (2007) 1720–1730.
- [6] M.Y. Iscan, Forensic anthropology of sex and body size, *Forensic Sci. Int.* 147 (2–3) (2005) 107–112.
- [7] K. Krishan, et al., A review of sex estimation techniques during examination of skeletal remains in forensic anthropology casework, *Forensic Sci. Int.* 261 (2016), 165 e1-8.
- [8] J. Bruzek, A method for visual determination of sex, using the human hip bone, *Am. J. Phys. Anthropol.* 117 (2) (2002) 157–168.
- [9] S.J. Decker, et al., Virtual determination of sex: metric and nonmetric traits of the adult pelvis from 3D computed tomography models, *J. Forensic Sci.* 56 (5) (2011) 1107–1114.
- [10] P.L. Walker, Greater sciatic notch morphology: sex, age, and population differences, *Am. J. Phys. Anthropol.* 127 (4) (2005) 385–391.
- [11] J. Bruzek, Fiabilité des fonctions discriminantes dans la détermination sexuelle de l'os coxal. Critiques et propositions, *Bull. Et. Mémoires De. la Société D. 'Anthropol. De. Paris* 4 (1) (1992) 67–104.
- [12] J. Bruzek, et al., Validation and reliability of the sex estimation of the human os coxae using freely available DSP2 software for bioarchaeology and forensic anthropology, *Am. J. Phys. Anthropol.* 164 (2) (2017) 440–449.
- [13] S. Genovés, L'estimation des différences sexuelles dans l'os coxal: différences métriques et différences morphologiques, *Bull. Et. Mémoires De. la Société D. 'Anthropol. De. Paris* 10 (1) (1959) 3–95.
- [14] P.N. Gonzalez, V. Bernal, S.I. Perez, Geometric morphometric approach to sex estimation of human pelvis, *Forensic Sci. Int.* 189 (1–3) (2009) 68–74.
- [15] P. Murrail, et al., DSP: a tool for probabilistic sex diagnosis using worldwide variability in hip-bone measurements, *Bull. Et. mémoires De. la Société d'Anthropologie De. Paris. BMSAP* 17 (17 (3–4)) (2005) 167–176.
- [16] C. Abegg, et al., Virtual anthropology: a preliminary test of macroscopic observation versus 3D surface scans and computed tomography (CT) scans, *Forensic Sci. Res.* 6 (1) (2021) 34–41.
- [17] S. Braun, et al., What we see is what we touch? Sex estimation on the pelvis in virtual anthropology, *Int. J. Leg. Med.* (2023) 1–14.
- [18] K.L. Colman, et al., The accuracy of 3D virtual bone models of the pelvis for morphological sex estimation, *Int. J. Leg. Med.* 133 (6) (2019) 1853–1860.
- [19] A. DesMarais, Z. Obertova, D. Franklin, Validation of DSP2 in an Australian sample of pelvic CT scans. *Fase Basic Course and Symposium 2022*, University of Crete, 2022.
- [20] I. Jerkovic, et al., The repeatability of standard cranial measurements on dry bones and MSCT images, *J. Forensic Sci.* 67 (5) (2022) 1938–1947.
- [21] R. Omari, et al., Virtual anthropology? Reliability of three-dimensional photogrammetry as a forensic anthropology measurement and documentation technique, *Int. J. Leg. Med.* 135 (3) (2021) 939–950.
- [22] Hoxha, F., et al. The Digital Era: Virtual Anthropology or: The reliability of sex estimation methods in a virtual environment (CT and 3D) using Probabilistic Sex Diagnosis (DSP) and Ischio-Pubic Index (IPI). in *Annual meeting of the Swiss Society for Anthropology*. 2022. Basel.
- [23] Perreard Lopreno, G., *Les collections ostéologiques humaines du Département d'anthropologie et d'écologie de l'Université de Genève*. 2006: Assoc. Provence Archéologie.
- [24] A.H. Schultz, The skeleton of the trunk and limbs of higher primates, *Hum. Biol.* 2 (3) (1930) 303–438.
- [25] S.L. Washburn, Sex differences in the pubic bone, *Am. J. Phys. Anthr.* 6 (2) (1948) 199–207.
- [26] R. Drew, A Review of the ischium-pubis index: accuracy, reliability, and common errors, *Hum. Biol.* 85 (4) (2013) 579–596.
- [27] D.H. Kim, et al., A new landmark for measuring the Ischium-Pubis index for sex determination by using three-dimensional models of South Korean population, *Aust. J. Forensic Sci.* 50 (5) (2018) 472–481.
- [28] G. Bräuer, Osteometrie, Sonderdruck Band 1/1: Wesen und Methoden der Anthropologie, in: R. Knußmann (Ed.), *Anthropologie: Handbuch der vergleichenden Biologie des Menschen*, zugleich 4, Auflage der Lehrbuchs der Anthropologie, begr. von Rudolf Martin, Gustav Fischer Verlag, Stuttgart-New York, 1988.
- [29] J. Gaillard, Détermination sexuelle d'un os coxal fragmentaire, *Bull. Et. Mémoires De. la Société D. 'Anthropol. De. Paris* 1 (2) (1960) 255–267.
- [30] F. Schultzer-Ellis, et al., Determination of sex with a discriminant analysis of new pelvic bone measurements: Part I, *J. Forensic Sci.* 28 (1) (1983) 169–180.
- [31] T.A. Perini, et al., Technical error of measurement in anthropometry, *Rev. Bras. De. Med. do Esport.* 11 (2005) 81–85.
- [32] I.E. Dror, N. Scirich, (Mis)use of scientific measurements in forensic science, *Forensic Sci. Int. Synerg* 2 (2020) 333–338.
- [33] Z.B. Popović, J.D. Thomas, Assessing observer variability: a user's guide, *Cardiovasc. Diagn. Ther.* 7 (3) (2017) 317–324.
- [34] S.J. Ulijaszek, D.A. Kerr, Anthropometric measurement error and the assessment of nutritional status, *Br. J. Nutr.* 82 (3) (1999) 165–177.
- [35] T. Chapman, et al., Sex determination using the Probabilistic Sex Diagnosis (DSP: Diagnose Sexuelle Probabiliste) tool in a virtual environment, *Forensic Sci. Int.* 234 (2014), 189 e1-8.
- [36] S. Mestekova, et al., A test of the DSP Sexing Method on CT images from a modern french sample, *J. Forensic Sci.* 60 (5) (2015) 1295–1299.
- [37] G. Quatrehomme, et al., Sex determination using the DSP (probabilistic sex diagnosis) method on the coxal bone: Efficiency of method according to number of available variables, *Forensic Sci. Int.* 272 (2017) 190–193.
- [38] L.F. Campana, S. Moghaddam, N. Grabherr, Comment to "AJ Collings, K. Brown, reconstruction and physical fit analysis of fragmented skeletal remains using 3D imaging and printing, *Forensic Sci. Int. Rep.* (2021).
- [39] S. Fahrni, et al., CT-scan vs. 3D surface scanning of a skull: first considerations regarding reproducibility issues, *Forensic Sci. Res* 2 (2) (2017) 93–99.
- [40] S. Grabherr, et al., Estimation of sex and age of "virtual skeletons"- a feasibility study, *Eur. Radiol.* 19 (2) (2009) 419–429.
- [41] M.G.P. Cavalcanti, S.S. Rocha, M.W. Vannier, Craniofacial measurements based on 3D-CT volume rendering: implications for clinical applications, *Dentomaxillofacial Radiol.* 33 (3) (2004) 170–176.
- [42] K.E. Stull, et al., Accuracy and reliability of measurements obtained from computed tomography 3D volume rendered images, *Forensic Sci. Int.* 238 (2014) 133–140.
- [43] K.R. Burns. *Forensic Anthropology Training Manual*, Second ed., Pearson Education, Inc, Upper Saddle River, New Jersey, USA, 2007.
- [44] A.M. Christensen, N.V. Passalacqua, E.J. Bartelink, *Forensic Anthropology: Current Methods and Practice*, *Forensic Anthropol.: Curr. Methods Pract.* (2014) 1–448.
- [45] Delabarde, T., B. Ludes, P. Adalian, *Manuel pratique d'anthropologie médico-légale*. 2014: Eska.
- [46] Obertová, Z., A. Stewart, C. Cattaneo, *Statistics and probability in forensic anthropology*. 2020: Academic Press.
- [47] Williams, L.L. and K. Quave, *Quantitative anthropology: a workbook*. 2019: Academic Press.
- [48] M. Bozdog, et al., Sex estimation in a modern Turkish population using the clavicle: a computed tomography study, *Aust. J. Forensic Sci.* 54 (2) (2022) 187–198.
- [49] S. Grabherr, et al., Multi-phase post-mortem CT angiography: development of a standardized protocol, *Int. J. Leg. Med.* 125 (6) (2011) 791–802.
- [50] K.L. Colman, et al., The geometrical precision of virtual bone models derived from clinical computed tomography data for forensic anthropology, *Int. J. Leg. Med.* 131 (4) (2017) 1155–1163.
- [51] S. de Froidmont, et al., Virtual anthropology: a comparison between the performance of conventional X-ray and MDCT in investigating the trabecular structure of long bones, *Forensic Sci. Int.* 225 (1–3) (2013) 53–59.
- [52] N.A. Ismail, et al., Accuracy and reliability of virtual femur measurement from CT scan, *J. Forensic Leg. Med.* 63 (2019) 11–17.
- [53] M.S. Reynolds, et al., Standardized anthropological measurement of postcranial bones using three-dimensional models in CAD software, *Forensic Sci. Int.* 278 (2017) 381–387.